Brief Articles

Structure-Based Design, Synthesis, and Biological Evaluation of Novel Pyrrolyl Aryl Sulfones: HIV-1 Non-Nucleoside Reverse Transcriptase Inhibitors Active at Nanomolar Concentrations

Marino Artico,*[,#] Romano Silvestri,[#] Eugenia Pagnozzi,[#] Biancamaria Bruno,[#] Ettore Novellino,[‡] Giovanni Greco,[‡] Silvio Massa,[§] Alessandro Ettorre,[†] Anna Giulia Loi,[||] Franca Scintu,[||] and Paolo La Colla*[,||]

Istituto Pasteur-Fondazione Cenci Bolognetti, Dipartimento di Studi Farmaceutici, Università degli Studi di Roma "La Sapienza", P.le A. Moro 5, BOX 36 - ROMA 62, I-00185 Roma, Italy, Dipartimento di Chimica Farmaceutica e Tossicologica, Università degli Studi di Napoli "Federico II", Via D. Montesano 49, I-80131 Napoli, Italy, Dipartimento Farmaco Chimico Tecnologico, Università degli Studi di Siena, Banchi di Sotto 55, I-53100 Siena, Italy, Menarini Ricerche SpA, Via T. Speri 10, 00040 Pomezia, Roma, Italy, and Dipartimento di Biologia Sperimentale, Sezione di Microbiologia, Università degli Studi di Cagliari, Cittadella Universitaria, SS 554, I-09042 Monserrato (Cagliari), Italy

Received March 12, 1999

Pyrrolyl aryl sulfones (PASs) have been recently reported as a new class of human immunodeficiency virus type 1 (HIV-1) reverse transcriptase (RT) inhibitors acting at the non-nucleoside binding site of this enzyme (Artico, M.; et al. *J. Med. Chem.* **1996**, *39*, 522−530). Compound **3**, the most potent inhibitor within the series (EC_{50} = 0.14 μM, IC_{50} = 0.4 μM, and SI > 1429), was then selected as a lead compound for a synthetic project based on molecular modeling studies. Using the three-dimensional structure of RT cocrystallized with the α-APA derivative R95845, we derived a model of the RT/**3** complex by taking into account previously developed structure−activity relationships. Inspection of this model and docking calculations on virtual compounds prompted the design of novel PAS derivatives and related analogues. Our computational approach proved to be effective in making qualitative predictions, that is in discriminating active versus inactive compounds. Among the compounds synthesized and tested, **20** was the most active one, with EC_{50} = 0.045 μM, IC_{50} = 0.05 μM, and SI = 5333. Compared with the lead **3**, these values represent a 3- and 8-fold improvement in the cell-based and enzyme assays, respectively, together with the highest selectivity achieved so far in the PAS series.

Introduction

Anti-HIV activity of sulfones was discovered at the National Cancer Institute (NCI) in 1993 following a large-scale drug-screening program on synthetic and natural products from a wide variety of sources. McMahon et al. reported the inhibition of HIV-1 reverse transcription by various diaryl sulfones and selected 2-nitrophenyl phenyl sulfone (**1**, NPPS; Chart 1), a potent inhibitor of reverse transcriptase (RT), as a lead compound for further investigations.[1] At the same time, screening of the drug repositories of Merck Research Laboratories led to the identification of 2-[(phenylsulfinyl)methyl]-3-(phenylthio)indole as a potent and specific inhibitor of HIV-1 RT. Attempts to optimize this compound with introduction of a chlorine atom and by oxidation of the sulfur atom to the corresponding sulfone gave the highly potent 5-chloro-3-(phenylsulfonyl)indole-2-carboxamide (**2**, L-737,126).[2] These findings indicated diaryl sulfones as a new emerging class of non-nucleoside reverse transcriptase inhibitors (NNRTIs) and gave great support to the idea of developing novel synthetic sulfones as inhibitors of RT. We therefore synthesized a number of pyrrolyl aryl sulfones (PASs) and reported on the anti-HIV-1 activities of these novel derivatives.[3] 2-Nitroaryl 2-ethoxycarbonyl-1*H*-pyrrolyl sulfones were identified as the most active among the first-generation series studied by us in 1995.

Chart 1. Sulfone Anti-HIV-1 Agents

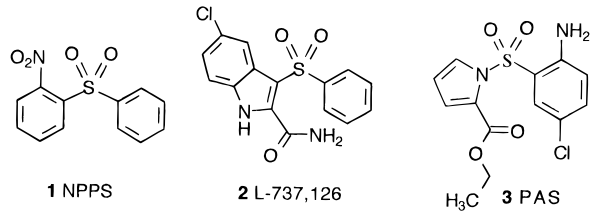

1 NPPS **2** L-737,126 **3** PAS

More recently, a second generation of PASs, characterized by a *p*-chloroaniline pharmacophore and targeted at RT, was found to exert higher and more specific anti-HIV-1 activity in vitro.[4] Compound **3** exhibited the highest activity within the series (EC_{50} = 0.14 μM, CC_{50} > 200 μM, IC_{50} = 0.4 μM, and SI > 1429). As a further development of the PAS series, we selected **3** as a lead compound for a synthetic project guided by structure-based molecular design.

* To whom correspondence should be sent. For M.A.: tel, 39-6-446-2731; e-mail, artico@uniroma1.it.
[#] Università degli Studi di Roma "La Sapienza".
[‡] Università degli Studi di Napoli "Federico II".
[§] Università degli Studi di Siena.
[†] Menarini Ricerche SpA.
[||] Università degli Studi di Cagliari.

10.1021/jm9901125 CCC: $19.00
Published on Web 04/14/2000

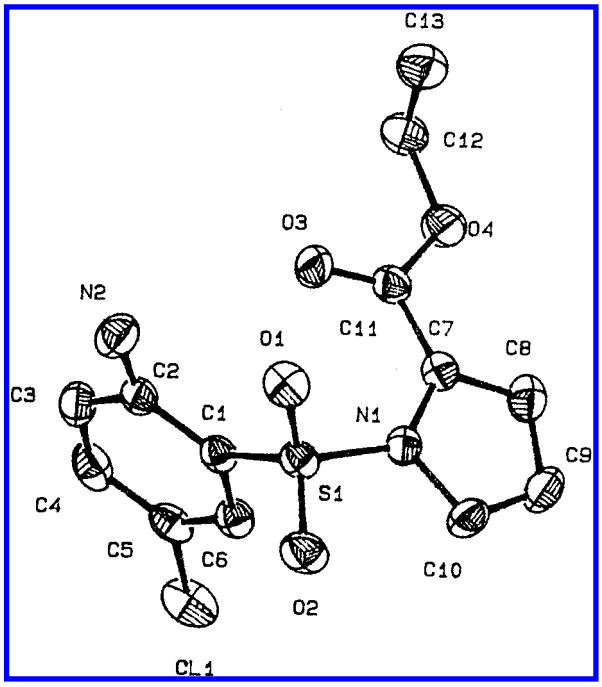

Figure 1. Crystal structure of compound **3** showing the thermal ellipsoids at 40% probability and the labeling of non-H atoms.

X-ray Crystallography of the Lead Compound 3

It is commonly recognized that the bioactive conformation of a ligand does not necessarily correspond to the lowest-energy conformation either in vacuo, in solution, or in a crystal. On the other hand, it can be reasonably assumed that the solid-state conformation is energetically stable and therefore not too far from the energy of the global minimum conformer in vacuo. On the basis of this assumption, strain energies of a given ligand can be estimated by taking the corresponding crystal structure as a bench mark. Accordingly, we determined the crystal geometry of the lead compound **3** to evaluate the strain energy of the enzyme-bound conformation of this inhibitor resulting from docking calculations. Strain energies not greater than 3−5 kcal/mol, typically calculated using molecular mechanics force fields or quantum-mechanics semiempirical methods, are usually regarded as "acceptable" values for a biological relevant conformation. A further advantage of having available the crystal structure of **3** was the possibility to check the calculated geometries of PAS derivatives and analogues about the sulfonamide moiety. In fact, this fragment is not adequately parametrized within the Tripos[6] and other molecular mechanics force fields.

Figure 1 shows the crystal structure of **3**, solved by X-ray diffraction methods as detailed in the Experimental Section. The values of the most relevant torsion angles defining the conformation of **3** are the following (see atom labeling in Figure 2): τ(C2−C1−S1−N1) = −128.7°, τ(C2−C1−S1−O1) = −12.8°, τ(C1−S1−N1−C7) = 62.8°, τ(N1−C7−C11−O4) = −179.5°, and τ(C11−O4−C12−C13) = 84.5°. The two aromatic rings of this compound are arranged in a propeller-like orientation.

Structure-Based Design

The design of new PAS derivatives was guided by a model of interaction between the lead compound **3** and the non-nucleoside binding site (NNBS) of RT. All calculations were performed using molecular mechanics (Tripos force field[5]), conformational analysis, and docking and graphics routines available within the SYBYL program.[6]

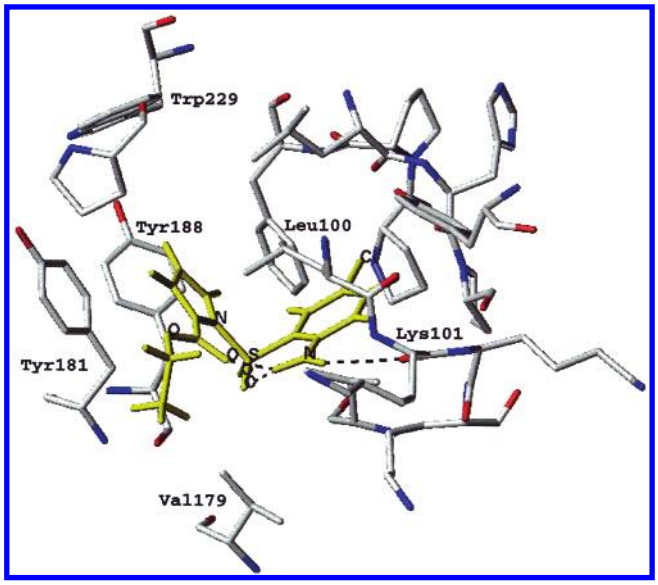

Figure 2. Lead compound **3** (yellow) docked into the NNBS of RT. Only a subset of residues closest to the ligand is displayed for sake of clarity.

The experimentally determined RT-bound conformations of α-APA R90385[7] served as a template to select a trial conformation of **3** for docking studies. By scanning the N1−S1 and S1−C1 rotatable bonds of the crystal structure of **3** (Figure 1), we identified a low-energy conformation of this compound superimposable on α-APA R95845 about the aromatic rings and the COOEt/COMe and SO_2/$CONH_2$ moieties. It will be shown that the proposed alignment enables the NH_2 of **3** to make a H-bond with the carbonyl oxygen of Lys101 within the NNBS. The same H-bond is crucial for the binding of NNRTIs such as HEPT[7,8] and TIBO[9,10] analogues.

The pharmacophore-based conformation of **3** was then placed into the NNBS taken from the crystal structure of the RT/α-APA R90385 complex[7] (filed in the Brookhaven Protein Data Bank[11] with the entry code 1VRU). A limited energy minimization of the RT/**3** complex, aimed at relieving steric repulsive contacts, did not modify significantly the starting geometry. The internal energy of the docked inhibitor resulted in 2.3 kcal/mol greater than that of the corresponding crystal structure.

Our model of the RT/**3** complex is depicted in Figure 2. As stated, the NH_2 group of the inhibitor forms a H-bond with the carbonyl oxygen of Lys101, thus rationalizing SARs of previously reported PAS derivatives:[4] (i) removal of NH_2 or its replacement with a NO_2 strongly lowers antiviral activity; (ii) removal of *p*-chlorine as well as its replacement with a *p*-methyl disfavors activity probably owing to electronic effects exerted by the *para*-substituent on the H-bond donor character of the NH_2. Two intramolecular H-bonds, donated by the NH_2 to the sulfone and ester oxygens, stabilize the bound conformation of **3**.

The solid-state and docked conformations of **3** differ in the values of the torsion angles τ(C2−C1−S1−N1), τ(C1−S1−N1−C7), τ(N1−C7−C11−O4), and τ(C11−

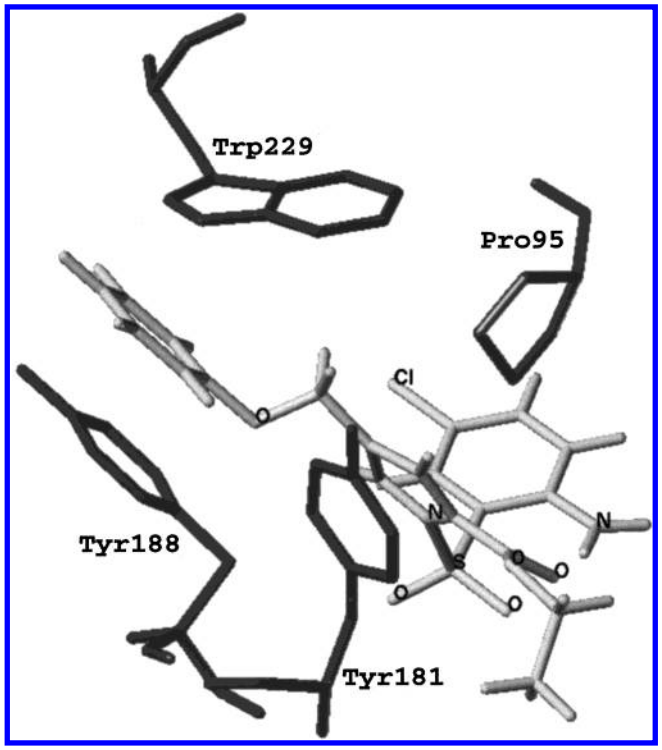

Figure 3. Theoretical model of the RT/**24** complex characterized by attractive interactions between the terminal phenyl ring of the docked molecule (gray) and the side chains of Tyr188 and Trp 229. Only four residues of the NNBS (black) are displayed.

O4−C12−C13): −128.7° vs 98.9°, 62.8° vs −104.2°, −179.5° vs −162.9°, and 84.5° vs −71.5°, respectively (see Figure 1 for atom labeling). In both conformations one of the SO_2 oxygens is eclipsed with the plane of the benzene ring and accepts a H-bond from the NH_2. In the crystal geometry the two aromatic rings are in a propeller-like disposition, whereas the same rings assume a butterfly-like arrangement in the proposed bioactive conformation.

An inspection of the RT/**3** complex (Figure 3) revealed a region of the NNBS, delimited by Tyr181, Tyr188, and Trp229 side chains, which could be filled by substituents at the 4-position of the inhibitor pyrrole ring. Accordingly, we introduced at this position small to medium size groups such as methyl, hydroxymethyl, α-hydroxyethyl, vinyl, and methoxymethyl (compounds **18**, **20**−**23**, and **25**). Phenoxymethyl and anilinomethyl substituents at the 4-position of the pyrrole were also considered prompted by results of docking calculations on the molecular models of **24**, **26**, and **27**. As shown in Figure 3, the terminal phenyl ring of **24** was hypothesized to favorably contact the Tyr188 (with a π-stacking interaction) and Trp229 side chains.

To evaluate our theoretical model to discriminate between active versus inactive PAS derivatives, two structures predicted to be inactive ("negative controls") were synthesized and tested as well: the 6-chloro-2-aminophenyl and 5-chloro-2-(1*H*-pyrrol-1-yl)phenyl derivatives **19** and **28**, respectively. Molecular mechanics calculations on **19** revealed that this structure could not attain the pharmacophoric butterfly-like conformation due to an intramolecular steric clash between the chlorine and the hydrogen on the 5-position of the

Chart 2. Newly Synthesized Pyrrolyl Aryl Sulfones

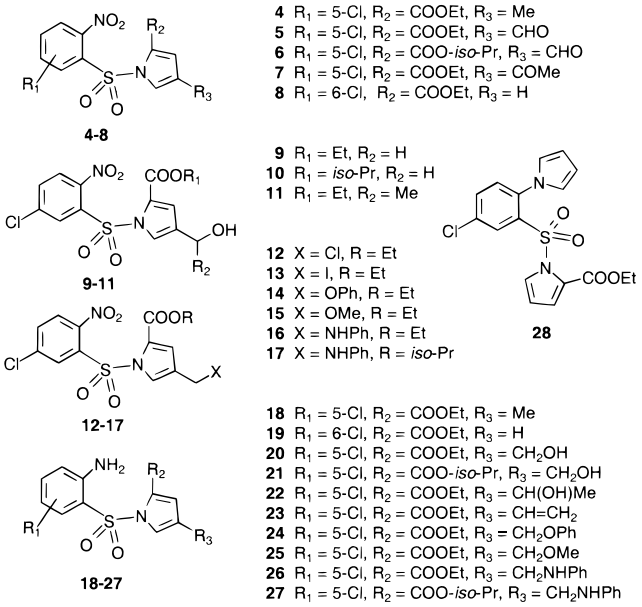

pyrrole ring. Concerning **28**, it was anticipated that an intermolecular steric repulsion between the bulky 2-pyrrolyl substituent on the phenyl ring and the carbonyl group of Lys101 would prevent the binding to RT.

Chemistry

Sulfones **4**−**8** (Chart 2) were prepared according to previously reported procedures by phase-transfer condensation of arylsulfonyl chlorides with the appropriate pyrroles in the presence of 18-crown-6 and potassium *tert*-butoxide.

Sodium borohydride reduction of **5**−**7** afforded the corresponding alcohols **9**−**11.** Treatment of **9** with phosphorus pentachloride gave **12**, which in turn was transformed into the more reactive iodide **13**. Reaction of the last compound with phenol in alkaline medium gave the required ethyl 1-[(5-chloro-2-nitrophenyl)-sulfonyl]-4-phenoxymethyl-1*H*-pyrrole-2-carboxylate (**14**). Similarly **13** was transformed into **15** by reaction with methanol.

Condensation of **5** and **6** with aniline followed by sodium cyanoborohydride reduction of the intermediate azomethines afforded ethyl (**16**) and isopropyl 1-[(5-chloro-2-nitrophenyl)sulfonyl]-4-phenylaminomethyl-1*H*-pyrrole-2-carboxylate (**17**), respectively.

Transformation of nitro derivatives **4**, **8**−**11**, and **14**−**17** into the corresponding amino sulfones **18**−**22** and **24**−**27**, respectively, was reached by heating at 60 °C with iron powder in glacial acetic acid. Ethyl 1-[(2-amino-5-chlorophenyl)sulfonyl]-1*H*-pyrrole-2-carboxylate (**3**)[4] was reacted with 2,5-dimethoxytetrahydrofuran via the Clauson−Kaas pyrrole synthesis to give **28**.

1-[(2-Amino-5-chlorophenyl)sulfonyl]-4-(1-hydroxyethyl)-1*H*-pyrrole-2-carboxylate (**22**) was transformed into ethyl 1-[(2-amino-5-chlorophenyl)sulfonyl]-4-vinyl-1*H*-pyrrole-2-carboxylate (**23**) by heating at 100 °C in the presence of phosphorus pentoxide.

The chemical and physical data of novel pyrrolyl aryl sulfones are reported in Table 1.

Results and Discussion

Aryl pyrrolyl sulfones **18**−**28** were assayed for cytotoxicity and anti-HIV-1 activity. Most of the compounds

Table 1. Chemical and Physical Data of Compounds **4**−**28**[a]

compd	formula	mp (°C)	crystal[b] from	yield (%)	chromat[c] system
4	$C_{14}H_{13}N_2O_6SCl$	150−151	A	63	a
5	$C_{14}H_{11}N_2O_7SCl$	191−192	B	64	a
6	$C_{15}H_{13}N_2O_7SCl$	179	B	70	a
7	$C_{15}H_{13}N_2O_7SCl$	163−164	B	72	a
8	$C_{13}H_{11}N_2O_6SCl$	151−153	B	28	a
9	$C_{14}H_{13}N_2O_7SCl$	147−150	C	68	b
10	$C_{15}H_{15}N_2O_7SCl$	155−156	B	69	b
11	$C_{15}H_{15}N_2O_7SCl$	107−108	C	69	c
12	$C_{14}H_{12}N_2O_6SCl_2$	135−136	B	78	a
13	$C_{14}H_{12}N_2O_6SClI$	144−145	C	100	a
14	$C_{20}H_{17}N_2O_7SCl$	124−125	C	43	a
15	$C_{15}H_{15}N_2O_7SCl$	92−93	A	35	a
16	$C_{20}H_{18}N_3O_6SCl$	98−99	C	96	a
17	$C_{21}H_{20}N_3O_6SCl$	105−106	C	92	a
18	$C_{14}H_{15}N_2O_4SCl$	148−149	B	73	a
19	$C_{13}H_{13}N_2O_4SCl$	103−104	A	90	a
20	$C_{14}H_{15}N_2O_5SCl$	151−152	B	95	b
21	$C_{15}H_{17}N_2O_5SCl$	140−142	B	69	c
22	$C_{15}H_{17}N_2O_5SCl$	123−124	C	80	c
23	$C_{15}H_{15}N_2O_4SCl$	123	D	32	a
24	$C_{20}H_{19}N_2O_5SCl$	129−131	C	98	a
25	$C_{15}H_{17}N_2O_5SCl$	95−98	A	68	b
26	$C_{20}H_{20}N_3O_4SCl$	147−148	C	98	a
27	$C_{21}H_{22}N_3O_4SCl$	129−130	C	61	a
28	$C_{17}H_{16}N_2O_4S$	102−103	D	98	a

[a] Analyzed elements: C, H, N, S and, when present, Cl, F. Analytical results where within ±0.4% of the theoretical values. [b] A, cylohexane; B, toluene−cyclohexane; C, toluene−ligroin. [c] a, silica gel/chloroform; b, silica gel/chloroform−ethanol (9:1); c, silica gel/ethyl acetate.

Table 2. Cytotoxicity, Anti-HIV-1 Activity in MT-4 Cells, Selectivity Index, and RT Inhibitory Activity of PASs **18**−**28**[a]

compd	CC_{50}[b]	EC_{50}[c]	SI[d]	IC_{50}[e]
18	>200	0.09	>2222	0.08
19	180	72	2.5	>100
20	240	0.045	5333	0.05
21	116	0.1	1160	0.11
22	115	0.25	460	0.17
23	47	0.17	274	0.28
24	>200	4.1	>49	0.6
25	>200	0.4	>500	0.6
26	>200	3.1	>55.5	0.5
27	40	0.2	200	0.3
28	110	>110		>100
3	>200	0.14	>1429	0.4
nevirapine	>200	0.35	>571	0.64

[a] Data represent mean values for three separate experiments. [b] Variation among triplicate samples was less than 15%. Compound dose (μM) required to reduce the viability of mock-infected cells by 50% as determined by the MTT method. [c] Compound dose (μM) required to achieve 50% protection of MT-4 cells from HIV-1-induced cytopathicity as determined by MTT method. [d] Selectivity index, CC_{50}/EC_{50} ratio. [e] Compound dose (mM) required to inhibit the HIV-1 rRT activity by 50%.

were also tested against wild-type recombinant reverse transcriptase (rRT). Table 2 summarizes the results of the biological evaluations, expressed as CC_{50} (cytotoxicity), EC_{50} (anti-HIV-1 activity), SI (selectivity), and IC_{50} (RT inhibitory activity) values.

As predicted using our model of the RT/**3** complex, the insertion of small to medium size substituents, such as methyl (**18**), hydroxymethyl (**20**, **21**), or α-hydroxyethyl (**22**) on the pyrrole 4-position led to inhibitors more active than their parent compound **3**. The most active one was **20**, which exhibited anti-HIV-1 and enzymatic inhibitory activities at nanomolar concentrations (EC_{50} = 45 nM and IC_{50} = 50 nM), with low cytotoxicity (CC_{50} = 240 μM) and high selectivity (SI = 5333). Compared with nevirapine, this compound was more active in the cell-based assay against HIV-1 (8-fold) and as a RT inhibitor (12-fold).

Derivatives substituted at the same position with methoxymethyl (**25**) or vinyl (**23**) were as active as **3**. Introduction of phenoxymethyl (**24**) and anilinomethyl groups (**26**, **27**) at the pyrrole 4-position produced RT inhibitors with IC_{50} values comparable with that of the lead compound **3**.

Finally, the importance of the *p*-chloroaniline pharmacophore was confirmed by the inactivity of the *m*-chloroaniline and 5-chloro-2-pyrrolylphenyl derivatives **19** and **28**, respectively. Indeed, we predicted that these two compounds would be inactive: the former is unable to attain the required "butterfly-like" conformation,[7−9] while the latter does not make the supposedly vital H-bond with the Lys101 carbonyl.

In conclusion, a theoretical model of interaction between the lead compound **3** and the NNBS of RT, consistent with previously developed SARs, was employed to design novel PAS derivatives and analogues. Our approach succeeded in optimizing activity of the lead as well as in discriminating active versus inactive molecules prior to their synthesis and biological evaluation. Among the compounds synthesized and tested, **20** turned out as the most active, with a 3- and 8-fold improvement over the lead **3** in the cell-based and enzyme assays, respectively.

Experimental Section

For general experimental information, see ref 5. Usual workup: the mixture reaction was concentrated and extracted with ethyl acetate; the collected extracts were washed with brine, dried on anhydrous sodium sulfate, and evaporated under reduced pressure.

General Procedure for the Condensation of Arylsulfonyl Chlorides with 1*H*-Pyrrole-2-carboxylates: Example − Ethyl 1-[(5-Chloro-2-nitrophenyl)sulfonyl]-4-methyl-1*H*-pyrrole-2-carboxylate (4). Sulfones **4**−**8** were prepared by phase-transfer reaction as we reported in a previous paper[4] (Table 1).

General Procedure for the Reduction of Nitro Group to Amino: Example − Ethyl 1-[(2-Amino-5-chlorophenyl)sulfonyl]-4-methyl-1*H*-pyrrole-2-carboxylate (18). Sulfones **18**−**22** and **24**−**27** were prepared by reduction of the corresponding nitro derivatives as we reported in a previous paper[4] (Table 1).

General Procedure for the Reduction of Aldehyde or Ketone to Alcohol: Example − Ethyl 1-[(5-Chloro-2-nitrophenyl)sulfonyl]-4-hydroxymethyl-1*H*-pyrrole-2-carboxylate (9). Sodium borohydride (0.098 g, 0.0026 mol) was added in portions to a solution of **5** (1.00 g, 0.0026 mol) in THF (7.5 mL) containing 0.4 mL of water, then the mixture was refluxed for 2 h. Water (5 mL) was added to the cooled mixture while stirring for a few min. After concentration, the solution was extracted with ethyl acetate, washed with brine and dried. Removal of the solvent afforded a residue which was purified on silica gel column, eluting with chloroform−ethanol, 9:1. First fractions were collected and evaporated to give **9**. Further elution with the same solvent gave ethyl 4-hydroxymethyl-1*H*-pyrrole-2-carboxylate (18%). By this procedure were also prepared **10** and **11** (Table 1).

Ethyl 1-[(5-Chloro-2-nitrophenyl)sulfonyl]-4-chloromethyl-1*H*-pyrrole-2-carboxylate (12). Phosphorus pentachloride (95%, 4.14 g, 0.0188 mol) was added in small portions over a period of 15 min to an ice-cooled solution of **9** (2.65 g, 0.0068 mol) in chloroform (60 mL). After stirring at 0 °C for 1 h, then at room temperature overnight the reaction mixture was poured onto crushed ice and extracted with chloroform. Usual workup afforded **12**.

Ethyl 1-[(5-Chloro-2-nitrophenyl)sulfonyl]-4-iodomethyl-1*H*-pyrrole-2-carboxylate (13). A solution of sodium iodide (0.194 g, 0.0013 mol) in acetone (5 mL) was added to a solution of **12** (0.53 g, 0.0013 mol) in the same solvent (5 mL), then the mixture was refluxed for 30 min. After concentration the residue was extracted with chloroform, washed with brine and dried. Removal of the solvent afforded pure **13**.

Ethyl 1-[(5-Chloro-2-nitrophenyl)sulfonyl]-4-phenoxymethyl-1*H*-pyrrole-2-carboxylate (14). A mixture of **13** (0.5 g, 0.001 mol), phenol (0.094 g, 0.001 mol), potassium carbonate (0.138 g, 0.001 mol) and acetone (10 mL) was refluxed for 4 h. After cooling ethyl acetate and water were added by shaking. Usual workup gave a residue which was purified on silica gel column. First eluates (dichloromethane−petroleum ether, 1:1) were discarded; further elution with chloroform afforded **14**.

Ethyl 1-[(5-Chloro-2-nitrophenyl)sulfonyl]-4-methoxymethyl-1*H*-pyrrole-2-carboxylate (15). Prepared as reported for **14** from **13** (1.0 g, 0.002 mol), methanol (40 mL), diethyl ether (40 mL), anhydrous tetrahydrofuran (20 mL) and sodium hydrogen carbonate (0.19 g, 0.0026 mol) with stirring at room temperature for 3 days.

Ethyl 1-[(5-Chloro-2-nitrophenyl)sulfonyl]-4-phenylaminomethyl-1*H*-pyrrole-2-carboxylate (16) Sodium cyanoborohydride (0.36 g, 0.0057 mol) was added to an ice-cooled solution of **5** (1.47 g, 0.0038 mol) and aniline (0.46 g, 0.0049 mol) in methanol (50 mL) and THF (50 mL) containing 0.63 mL of a 6 N HCl/MeOH (1:1) solution. The reaction was stirred at 0 °C for 2 h, then at room temperature overnight. Usual workup gave a crude product which was chromatographed to afford **16**. By this procedure was also prepared **17** starting from **6**.

Ethyl 1-[(2-Amino-5-chlorophenyl)sulfonyl]-4-vinyl-1*H*-pyrrole-2-carboxylate (23). Phosphorus pentoxide (1.65 g, 0.0116 mol) was added by small portions to a stirred mixture of **22** (1.00 g, 0.0027 mol) in anhydrous benzene (30 mL), then reaction was heated at 100 °C for 45 min. After cooling the organic solution was separated and the gummy residue was extracted with benzene. Combined cloudy extracts were filtered, washed with 5% $NaHCO_3$ solution and then with brine and dried. After concentration the residue was chromatographed to yield **23**.

Ethyl 1-{[5-Chloro-2-(1*H*-pyrrol-1-yl)phenyl]sulfonyl}-1*H*-pyrrole-2-carboxylate (28). A solution of ethyl 1-(2-amino-5-chlorophenylsulfonyl)-1*H*-pyrrole-2-carboxylate (**3**) (1.00 g, 0.0034 mol) and 2,5-dimethoxytetrahydrofuran (90%, 0.90 g, 0.0061 mol) in glacial acetic acid (20 mL) was refluxed for 1 h, then evaporated to dryness. Usual workup gave **28** which was purified by chromatography.

Isopropyl 4-Formyl-1*H*-pyrrole-2-carboxylate. A solution of dichloromethyl methyl ether (13.80 g, 0.12 mol) in 1,2-dichloroethane (50 mL) was quickly added to a stirred mixture of isopropyl 1*H*-pyrrole-2-carboxylate (15.31 g, 0.10 mol) and anhydrous aluminum trichloride (32.00 g, 0.24 mol) in 1,2-dichloroethane (200 mL) while cooling at −30 °C, and the reaction was maintained at −30 °C overnight. After reaching 0 °C, the mixture was poured on ice water and extracted with chloroform. Organic extracts were combined, washed with brine and dried. Removal of the solvent gave a residue which was purified on a silica gel column (chloroform): yield 50%; mp 85−86 °C (toluene/cyclohexane). Anal. ($C_9H_{11}NO_3$) (181.19) C, H, N.

Methods. X-ray Crystallography of Compound 3. Single crystals of **3** suitable for X-ray diffraction analysis were obtained by recrystallization from a hot ethanol solution. All measurements were made on a Rigaku AFC5R diffractometer with graphite monochromated Cu Kα radiation and a rotating anode generator. The $\omega/2\theta$ scan tecnique was used. The structure was solved by direct methods; the positions of hydrogens were calculated and not refined. All calculations were performed using the TEXSAN crystallographic software package of Molecular Structure Corp.[12] The data for **3** were as follows: $C_{13}H_{13}N_2O_4SCl$, M_r 282.77, a = 7.9558(9) Å, b = 21.069(5) Å, c = 7.633(1) Å, β = 93.69(1)°, V = 1138.5(3) Å^3, Z = 4, space group $P21/a$ (No. 14), monoclinic, DC = 1.649 g/cm^{-3}, λ(Cu Kα) = 1.54178 Å, T = 293 K. A total of 2009 reflections were measured, 1853 of which were independent. The anisotropic refinement of the non-hydrogen atoms used 1468 observed reflections [$I > 3\sigma(I)$] and converged to R = 0.049, RW = 0.060, S = 1.98. Parameters refined 163, D_r in the final difference map was within +0.50 and −0.41 Å^3.

Molecular Modeling. Molecular modeling studies were performed using the SYBYL[6] software package running on a Silicon Graphics R8000 workstation. Intramolecular and intermolecular energies were calculated using the molecular mechanics Tripos force field[5] including the electrostatic contribution. Atom centered partial charges were calculated according to the Gasteiger−Hückel method.[13,14] Geometry optimizations were realized with the SYBYL/MAXIMIN2 minimizer by applying the BFGS algorithm[15] and setting a root-mean-square gradient of the forces acting on each atom at 0.05 kcal/mol Å as a convergence criterion.

Hydrogens were added to the unfilled valences of the crystal structure of compound **3** and their positions optimized while keeping fixed the rest of the molecule. The putative bioactive conformation of **3** was sought following a two-step approach: (i) selection of a pharmacophore-consistent conformation and (ii) docking of this latter into the NNBS of RT.

First, we identified a low-energy conformation of **3** superimposable on the experimentally determined bioactive conformation of the α-APA type inhibitor R90385 extracted from the RT/R90385 complex solved at 2.4 Å resolution.[7] The coordinates of this complex are filed in the Brookhaven Protein Data Bank[11] with the entry code 1VRU. The search for the pharmacophore-based conformation of **3** was performed by manual adjustment of the torsion angles about the N1−S1 and S1−C1 and rotatable bonds (see Figure 2 for atom labeling) aimed at finding a butterfly-like orientation of the two aromatic rings. As further constraints, we wanted to match the COOEt and COMe carbonyl oxygens of **3** and R90385, respectively, and orient the NH_2 group of **3** toward the Lys101 carbonyl oxygen as part of the NNBS. Compound **3** was overlayed on R90385 by minimizing the root-mean-square distance between the following five points: (i) pseudoatoms placed at 1.0 Å along the normals to the plane of each aromatic ring passing through the ring centroid; (ii) the SO_2 sulfur and the $CONH_2$ carbon. The energy of the resulting conformation of **3** was only 3.0 kcal/mol above that of the corresponding crystal geometry (this value was computed considering the sum of the nonbonded components of the force field, i.e., van der Waals plus electrostatics).

The resulting pharmacophore-based conformation of **3** was then placed into the NNBS extracted from the crystal structure of the RT/R90385 complex. The NNBS comprised 71 amino acids located within a distance of 10 Å from any non-hydrogen atom of the bound inhibitor. Water molecules were deleted. Hydrogens were added to the unfilled valences of the amino acids and the Lys, Asp and Glu side chains were modeled in their ionized forms. The torsion angle τ(C11−O4−C12−C13) of **3** was manually changed from 84.5° to −75.0° to avoid a steric clash between the ester group and the Leu100 side chain. The resulting NNBS/**3** complex was geometry-optimized by keeping fixed the coordinates of the protein backbone until an attractive intermolecular interaction energy of 25 kcal/mol was reached. The internal energy of the docked conformation rose by 2.3 kcal/mol with respect to the crystal structure.

Given the lack of adequate parametrization for the sulfonamide moiety featured by all the PAS derivatives, bond distances and bond angles of this fragment were kept fixed to the values measured in the crystal structure of **3** throughout the docking calculations. This was done by applying specific penalty functions characterized by strong force constants. The torsion angles of the sulfonamide residue were, in contrast, left free to vary as though they had no impact on the internal energy of the molecule (this was accomplished by setting the corresponding torsional force constants to zero). However, the geometry of the sulfonamide moiety in the docked conformation of the ligand was checked a posteriori against the crystal structures of **3** and of 31 pyrrolyl sulfone derivatives retrieved

from the Cambridge Structural Database (CSD)[16] by a substructure search. The 3D graphics 5.13 version of the CSD for UNIX platforms (April 1997 release) was employed. Analysis of these structures and of a published survey on sulfonamide crystal geometries[17] revealed that the combination of values assumed by the $C_{aryl}-N-S-C_{aryl}$ and $C_{aryl}-C_{aryl}-S-N$ torsion angles in the docked conformation of **3** was within the range of experimental values.

Models of derivatives and analogues of compound **3** were constructed starting from the docked conformation of **3** and submitted to geometry optimization of the resulting NNBS/inhibitor complex as described above.

In the case of the phenoxymethyl (**24**) and anilinomethyl (**26**) derivatives, molecular dynamics (MD) simulations of the corresponding complexes were performed with the SYBYL/DYNAMICS module under default settings. These simulations, in which the protein backbone was treated as a rigid aggregate, were run at 300 K for 50 ps after reaching equilibration. Five structures extracted at 10, 20, 30, 40 and 50 ps were selected and energy-minimized. Figure 3, displaying the interaction between the terminal phenyl ring of compound **24** and the side chains of Tyr188 and Trp229, refers to the last MD snapshot.

Antiviral Assays. HIV Titration. As previously reported[4] titration of HIV was performed in C8166 cells by the standard limiting dilution method (dilution 1:2, four replica wells/dilution) in 96-well plates. The infectious virus titer was determined by light microscope scoring of cytopathicity after 4 days of incubation and the virus titers were expressed as $CCID_{50}$/mL.

Anti-HIV Assays. Activity of the compounds against HIV-1 multiplication in acutely infected cells was based on the inhibition of virus-induced cytopathicity in MT-4 and C 8166 cells, respectively. According to the previously reported procedure,[4] the number of viable cells was determined by the 3-(4,5-dimethylthiazol-1-yl)-2,5-diphenyltetrazolium bromide (MTT) method. Cytotoxicity of the compounds was evaluated in parallel with their antiviral activity. It was based on the viability of mock-infected cells, as monitored by the MTT method.

RT Assays. Assays were performed as previously described.[4]

Acknowledgment. We thank the Italian Ministero della Sanità - Istituto Superiore di Sanità - XI Progetto AIDS 1997 (Grants 40A.0.06 and 40A.0.55) for financial support. The Italian MURST (40%) and Regione Autonoma della Sardegna (Progetto Biotecnologie) are also acknowledged for partial support.

References

(1) McMahon, J. B.; Gulakowsky, R. J.; Weislow, O. S.; Schoktz, R. J.; Narayanan, V. L.; Clanton, D. J.; Pedemonte, R.; Wassmundt, F. W.; Buckheit, R. W., Jr.; Decker, W. D.; White, E. L.; Bader, J. P.; Boyd, M. R. Diaryl sulfones, a New Chemical Class of Non-Nucleoside Antiviral Inhibitors of Human Immunodeficiency Virus Type 1 Reverse Transcriptase. *Antimicrob. Agents Chemother.* **1993**, *37*, 754−760.

(2) Williams, T. M.; Ciccarone, T. M.; MacTough, S. C.; Rooney, C. S.; Balani, S. K.; Condra, J. H.; Emini, E. A.; Goldman, M. E.; Greenlee, W. J.; Kauffman, L. R.; O'Brien, J. A.; Sardana, V. V.; Schleif, W. A.; Theoharides, A. D.; Anderson, P. S. 5-Chloro-3-(phenylsulfonyl)indole-2-carboxamide: A Novel, Non-Nucleoside Inhibitor of HIV-1 Reverse Transcriptase. *J. Med. Chem.* **1993**, *36*, 1291−1294.

(3) Artico, M.; Silvestri, R.; Stefancich, G.; Massa, S.; Pagnozzi, E.; Musiu, D.; Scintu, F.; Pinna, E.; Tinti, E.; La Colla, P. Synthesis of Pyrryl Aryl Sulfones Targeted at the HIV-1 Reverse Transcriptase. *Arch. Pharm. (Weinheim)* **1995**, *328*, 223−229.

(4) Artico, M.; Silvestri, R.; Massa, S.; Loi, A. G.; Corrias, S.; Piras, G.; La Colla, P. 2-Sulfonyl-4-chloroanilino Moiety: A Potent Pharmacophore for the Anti-Human Immunodeficiency Virus Type 1 Activity of Pyrrolyl Aryl Sulfones. *J. Med. Chem.* **1996**, *39*, 522−530.

(5) Clark, M.; Cramer, R. D., III; Van Opdenbosch, N. Validation of the General Purpose Tripos 5.2 Force Field. *J. Comput. Chem.* **1989**, *10*, 982−1012.

(6) SYBYL Molecular Modeling System (version 6.2); Tripos Inc., St. Louis, MO.

(7) Ren, J.; Esnouf, R.; Garman, E.; Somers, D.; Ross, C.; Kirby, I.; Keeling, J.; Darby, G.; Jones, Y.; Stuart, D.; Stammers, D. High-Resolution Structures of HIV-1 RT from four RT-Inhibitor Complexes. *Nat. Struct. Biol.* **1995**, *2*, 293−302.

(8) Hopkins, A. L.; Ren, J.; Esnouf, R. M.; Willcox, B. E.; Jones, E. Y.; Ross, C.; Miyasaka, T.; Walker, R. T.; Tanaka, H.; Stammers, D. K.; Stuart, D. I. Complexes of HIV-1 Reverse Transcriptase with Inhibitors of the HEPT Series Reveal Conformational Changes Relevant to the Design of Potent Non-Nucleoside Inhibitors. *J. Med. Chem.* **1996**, *39*, 1589−1600.

(9) Ding, J.; Das, K.; Moereels, H.; Koymans, L.; Andries, K.; Janssen, P. A. J.; Hughes, S. H., Arnold, E. Structure of HIV-1 RT/TIBO R 86183 Complex Reveals Similarity in the Binding of Diverse Nonnucleoside Inhibitors. *Nat. Struct. Biol.* **1995**, *2*, 407−415.

(10) Ren, J.; Esnouf, R.; Hopkins, A.; Ross, C.; Jones, Y.; Stammers, D.; Stuart, D. The structure of HIV-1 Reverse Transcriptase Complexed with 9-Chloro-TIBO: Lessons for Inhibitor Design. *Structure* **1995**, *3*, 915−926.

(11) Bernstein, F. C.; Koetzle, T. F.; Williams, G. J. B.; Meyer Jr., E. F.; Brice, M. D.; Rodgers, J. R.; Kennard, O.; Shimanouchi, T.; Tasumi, T. The Protein Data Bank: A Computer Based Archival File for Macromolecular Structures. *J. Mol. Biol.* **1977**, *112*, 535−542.

(12) TEXAN-TEXRAY Single-Crystal Structure Analysis Software (version 5.0, 1989); Molecular Structure Corp., The Woodlands, TX 77381.

(13) Gasteiger, J.; Marsili, M. Iterative Partial Equalization of Orbital Electronegativity. *Tetrahedron* **1980**, *36*, 3219−3228.

(14) Purcel, V. P.; Singer, J. A. A Brief Review and Table of Semiepirical Parameters Used in the Hückel Molecular Orbital Method. *J. Chem. Eng. Data* **1967**, *12*, 235−246.

(15) Head, J.; Zerner, M. C. A Broyden-Fletcher-Goldfarb-Shanno Optimization Procedure for Molecular Geometries. *Chem. Phys. Lett.* **1985**, *122*, 264−274.

(16) Allen, F. H.; Bellard, S. Brice, M. D.; Cartwright, B. A.; Doubleday: A.; Higgs, H.; Hummelink, T.; Hummelink-Peterd, B. G.; Kennard, O.; Motherwell, W. D. S.; Rodgers, J. R.; Watson, D. G. The Cambridge Crystallographic Data Centre: Computer-Based Search, Retrival, Analysis and Display of Information. *Acta Crystallogr.* **1979**, *B35*, 2331−2339.

(17) Krystek, Jr., S. R.; Hunt, J. T.; Stein, P. D.; Stouch, T. R. Three-Dimensional Quantitative Structure−Activity Relationships of Sulfonamide Endothelin Inhibitors. *J. Med. Chem.* **1995**, *38*, 659−668.

JM9901125